

Mechanism of Transducin Activation of Frog Rod Photoreceptor Phosphodiesterase

ALLOSTERIC INTERACTIONS BETWEEN THE INHIBITORY γ SUBUNIT AND THE NONCATALYTIC cGMP-BINDING SITES*

Received for publication, May 28, 2000, and in revised form, August 11, 2000
Published, JBC Papers in Press, September 18, 2000, DOI 10.1074/jbc.M004606200

Angela W. Norton, Marc R. D'Amours, Hector J. Grazio, Tracy L. Hebert, and Rick H. Cote‡

From the Department of Biochemistry and Molecular Biology, University of New Hampshire, Durham, New Hampshire 03824-3544

The rod photoreceptor phosphodiesterase (PDE) is unique among all known vertebrate PDE families for several reasons. It is a catalytic heterodimer ($\alpha\beta$); it is directly activated by a G-protein, transducin; and its active sites are regulated by inhibitory γ subunits. Rod PDE binds cGMP at two noncatalytic sites on the $\alpha\beta$ dimer, but their function is unclear. We show that transducin activation of frog rod PDE introduces functional heterogeneity to both the noncatalytic and catalytic sites. Upon PDE activation, one noncatalytic site is converted from a high affinity to low affinity state, whereas the second binding site undergoes modest decreases in binding. Addition of γ to transducin-activated PDE can restore high affinity binding as well as reducing cGMP exchange kinetics at both sites. A strong correlation exists between cGMP binding and γ binding to activated PDE; dissociation of bound cGMP accompanies γ dissociation from PDE, whereas addition of either cGMP or γ to $\alpha\beta$ dimers can restore high affinity binding of the other molecule. At the active site, transducin can activate PDE to about one-half the turnover number for catalytic $\alpha\beta$ dimers completely lacking bound γ subunit. These results suggest a mechanism in which transducin interacts primarily with one PDE catalytic subunit, releasing its full catalytic activity as well as inducing rapid cGMP dissociation from one noncatalytic site. The state of occupancy of the noncatalytic sites on PDE determines whether γ remains bound to activated PDE or dissociates from the holoenzyme, and may be relevant to light adaptation in photoreceptor cells.

Initiation of the phototransduction cascade in vertebrate rod photoreceptors by light results in the sequential activation of the visual pigment (rhodopsin), the photoreceptor G-protein (transducin), and the effector enzyme (cGMP phosphodiesterase (EC 3.1.4.35), PDE)¹ (for reviews see Refs. 1–4). The PDE

present in rod and cone photoreceptors (classified as PDE6) differs in several ways from other classes of mammalian phosphodiesterases (5–7): rod photoreceptor PDE forms a catalytic dimer from two closely related α and β subunits ($P\alpha\beta$); rod and cone PDE are directly regulated via heterotrimeric G-proteins. the catalytic constant (k_{cat}) for rod PDE is ~ 1000 -fold greater than for any other class of PDE; the catalytic activity of photoreceptor PDE is potently inhibited by binding of an inhibitory γ subunit ($P\gamma$) (for reviews see Refs. 8 and 9).

Transducin activation of PDE results from binding of the activated transducin α_t subunit (α_t -GTP) to one or more sites on the PDE holoenzyme. One result of this interaction is the displacement of the inhibitory $P\gamma$ subunit from its binding site in the catalytic pocket of PDE. It is not clear, however, whether each PDE catalytic subunit binds $P\gamma$ with equal affinity, whether α_t -GTP can activate each catalytic site equally well, and under what conditions the α_t -GTP- $P\gamma$ complex dissociates from $P\alpha\beta$. Conflicting results reported by different laboratories (10–24) may reflect underlying differences in how the phototransduction components were isolated and studied, as well as species differences in the protein-protein interactions of transducin and PDE.

Comparison of the amino acid sequence of photoreceptor PDE with PDE2, PDE5, PDE10, and PDE11 reveals the presence of GAF domains (25) in the N-terminal half of each PDE that encodes noncatalytic cGMP-binding sites (6, 7, 26–29). In the case of PDE2, cGMP binding to these noncatalytic sites directly stimulates cyclic nucleotide hydrolysis at the active site (30, 31). For PDE5, the noncatalytic sites allosterically regulate accessibility of a phosphorylation site that alters catalytic activity (32–34). The possible regulatory function for the low affinity, noncatalytic sites on PDE10 is not known, nor is it known whether the GAF domains in PDE 11 represent functional cGMP-binding sites.

Since the initial findings by Yamazaki *et al.* (35, 36) that cGMP bound with high affinity to rod photoreceptor PDE, several possible roles for the noncatalytic sites on rod PDE have been proposed. One hypothesis is that cGMP occupancy of the noncatalytic sites on PDE affects the strength of the interaction between the inhibitory $P\gamma$ subunit and $P\alpha\beta$ (reviewed in Ref. 9). It has also been proposed that changes in cGMP binding affinity to the noncatalytic sites during visual transduction might permit the release of bound cGMP to accelerate the restoration of cGMP levels during the recovery phase of the

* This work was supported by National Institutes of Health Grant EY-05798 (to R. H. C.). This paper is Scientific Contribution 2058 from the New Hampshire Agricultural Experiment Station. The costs of publication of this article were defrayed in part by the payment of page charges. This article must therefore be hereby marked "advertisement" in accordance with 18 U.S.C. Section 1734 solely to indicate this fact.

‡ To whom correspondence should be addressed: Dept. of Biochemistry and Molecular Biology, University of New Hampshire, 46 College Rd., Durham, NH 03824-3544. Tel.: 603-862-2458; Fax: 603-862-4013; E-mail: rick.cote@unh.edu.

¹ The abbreviations used are: PDE, phosphodiesterase from rod photoreceptors; $P\alpha\beta$, catalytic heterodimer of PDE; $P\gamma$, inhibitory 10-kDa γ subunit of rod PDE; α_t , α -subunit of the rod photoreceptor G-protein, transducin; ROS, rod outer segments; nPDE, nonactivated PDE; tPDE, trypsin-activated PDE; taPDE, transducin-activated PDE; GTP γ S,

guanosine 5'-O-[3-thiotriphosphate], α_t -GTP γ S, activated form of α_t ; k_{cat} , turnover number for activated PDE (units: cGMP hydrolyzed per s) based on the $P\alpha\beta$ dimer concentration; PDE1, calcium-calmodulin-dependent PDE.

photoresponse (37, 38). Finally, the idea that the noncatalytic sites on photoreceptor PDE might directly regulate hydrolysis of cGMP at the active site (as is the case for PDE2) has not been supported by current evidence (22, 39).

In this paper, we characterize the properties of non-activated, transducin-activated, and catalytic dimers of PDE, all derived from suspensions of purified amphibian rod outer segments, in order to provide a detailed account of the changes that occur at the catalytic and noncatalytic domains of PDE upon light activation of the phototransduction cascade. We demonstrate a direct correlation between occupancy of cGMP at the noncatalytic sites of PDE and the state of association of the inhibitory $P\gamma$ subunit. Our results are consistent with transducin activation reducing cGMP binding affinity primarily at one of the two high affinity, noncatalytic sites on PDE. Furthermore, transducin activation of PDE cannot achieve the maximum catalytic potential of PDE that is observed when the $P\gamma$ subunits are completely removed from the $P\alpha\beta$ catalytic dimer. These changes in the noncatalytic and catalytic sites upon transducin activation are mediated through changes in $P\gamma$ interaction with $P\alpha\beta$ upon binding of transducin to PDE. The coordinated, allosteric regulation of cGMP and $P\gamma$ binding to $P\alpha\beta$ upon transducin activation operate too slowly to play a role in the rapid events of rod phototransduction (*i.e.* excitation and recovery) but may be important in more slowly developing aspects of light adaptation.

EXPERIMENTAL PROCEDURES

Materials—Frogs (*Rana catesbeiana*) were obtained from Niles Biologicals. [^3H]cGMP was from PerkinElmer Life Sciences. Membranes for filter binding assays were obtained from Millipore. Reagents, substrates, and nitrocellulose membranes for immunoblotting were from Pierce or from Bio-Rad. Silicone oils for centrifugal separation were obtained from the William F. Nye Co. All other chemicals were obtained from Sigma.

Preparation of Frog Rod Outer Segments (ROS) and Recombinant Bovine Rod PDE Inhibitory γ Subunit ($P\gamma$)—Osmotically intact frog ROS were purified on a discontinuous Percoll density gradient exactly as described previously (40). Purified ROS were homogenized in Buffer A (containing 77 mM KCl, 35 mM NaCl, 2.0 mM MgCl_2 , 1.0 mM CaCl_2 , 10 mM HEPES (pH 7.5), 2 mM dithiothreitol, 1 mM 4-(2-aminoethyl)benzenesulfonyl fluoride, 5 μM leupeptin, and 1 $\mu\text{g}/\text{ml}$ pepstatin) following the method of Dumke *et al.* (21). Homogenized ROS were incubated in the dark at room temperature for 20–30 min to allow endogenous nucleotide hydrolases to degrade cGMP and GTP levels prior to experimental manipulations. Following depletion of nucleotides and determination of the rhodopsin concentration by difference spectroscopy (41), ROS samples were exposed to light for subsequent steps (unless otherwise noted). The PDE concentration in ROS homogenates was determined by its ability to bind a maximum of 2 mol of cGMP/mol of holoenzyme in its non-activated state when supplemented with stoichiometric amounts of exogenous $P\gamma$ (see Ref. 40 for details).

Subcellular fractionation of ROS homogenates was typically performed by centrifuging samples for 1–3 min at 30 pounds/square inch on the gauge ($110,000 \times g_{\text{av}}$) at room temperature using a Beckman Airfuge. We verified that the integral membrane protein, rhodopsin, was present in the supernatant at undetectable levels and that >95% of the total rhodopsin could be recovered in the membrane pellet under these conditions.

Recombinant bovine rod $P\gamma$ was expressed in *Escherichia coli* and purified to >97% purity as described in Ref. 42. The $P\gamma$ concentration was determined spectrophotometrically using an experimentally determined extinction coefficient of 7550 OD M^{-1} (40). The inhibitory activity of purified $P\gamma$ was assayed by its ability to inhibit stoichiometrically trypsin-activated bovine rod PDE (43); the spectrophotometric and activity estimates of $P\gamma$ concentration agreed to within 10% for all $P\gamma$ preparations used in this study.

PDE Preparations Used in This Study—Since PDE6 is the only detectable isoform of phosphodiesterase in purified ROS, no additional purification of the rod PDE was required. Non-activated PDE (nPDE) was obtained directly from nucleotide-depleted ROS homogenates; in the absence of GTP, dark-adapted and light-exposed ROS homogenates show no difference in the rate of cGMP hydrolysis or in the extent of

cGMP binding. The catalytic activity of nPDE was typically 1–3% of the activated rate at the concentrations used in this paper (22). Transducin-activated PDE (taPDE) was prepared by incubating nucleotide-depleted ROS homogenates ([PDE] ≥ 12 nM; see Ref. 21) with an excess of GTP- γS relative to the transducin concentration (~ 30 transducins per PDE (64)). Trypsinized PDE (tPDE), in which the $P\gamma$ subunits are proteolytically digested to relieve their inhibitory constraint (65), was prepared by incubating ROS homogenates with L-1-tosylamido-2-phenylethyl chloromethyl ketone-treated trypsin, followed by addition of a 6-fold molar excess of soybean trypsin inhibitor. The time course and concentration dependence of activation was closely followed to determine the minimum exposure of PDE to the protease yielding full activation (see “Results”). Excessive proteolysis of PDE leads to a gradual loss in the maximal catalytic activity, as well as irreversible damage to the noncatalytic sites. We prepared PDE heterodimers ($P\alpha\beta$) depleted of $P\gamma$ by modifying the original method of Yamazaki *et al.* (15); nPDE was incubated with GTP- γS for 60 min at 4 $^\circ\text{C}$ to allow $P\gamma$ to dissociate from $P\alpha\beta$ and then was centrifuged in the Airfuge to pellet ROS membranes. The supernatant was discarded, and the ROS membrane was treated with GTP- γS once more to release further membrane-bound $P\gamma$. Following the second centrifugation, ROS membranes retained all of the original $P\alpha\beta$ content but only 10–35% of the original $P\gamma$ (depending on the individual preparation). (The content of α_t in GTP- γS -washed ROS membranes was also reduced to <30% of its concentration in ROS homogenates, as judged by immunoblot analysis with anti- α_t antibodies.) $P\alpha\beta$ was used immediately following its preparation, because the enzyme was unstable once most of the $P\gamma$ had been removed. Only preparations containing <25% of the original $P\gamma$ content (*i.e.* <0.5 $P\gamma$ per PDE) were used in experiments employing $P\alpha\beta$. Efforts to eliminate completely $P\gamma$ from our $P\alpha\beta$ preparations were unsuccessful.

Binding of cGMP to Noncatalytic Sites on PDE—Because PDE is the only rod photoreceptor protein that binds cGMP with high affinity ($K_D < \mu\text{M}$) (37, 44), we were able to measure changes in binding occupancy at the noncatalytic sites of PDE in unfractionated ROS homogenates. For most experiments, a cGMP filter binding assay (40) was used to quantify binding of [^3H]cGMP to high affinity sites on PDE. Inclusion of zaprinast or E4021 (45) with the [^3H]cGMP solution during the filter binding assay prevented cGMP breakdown during the incubation with nPDE or activated PDE. In some experiments, the cGMP-binding reaction was halted by addition of ice-cold 95% saturated ammonium sulfate (40) prior to membrane filtration of the quenched samples.

In order to correlate directly cGMP binding with $P\gamma$ binding to activated PDE (shown in Fig. 4), we employed a centrifugal separation assay through a silicone oil layer that partitions free [^3H]cGMP from bound nucleotide (40, 46). Portions (10 μl) of ROS homogenates were layered on top of 100 μl of silicone oil (density, 1.020 g/ml) in a 5 \times 20-mm centrifuge tube (Beckman) at 4 $^\circ\text{C}$. The tubes were spun at room temperature for 3 min at $110,000 \times g_{\text{av}}$. Supernatants remaining above the oil layer were removed and processed for immunoblot analysis of $P\gamma$ concentration. The pellets were resuspended, and one portion was analyzed for $P\gamma$ content, whereas the other portion was used to quantitate bound [^3H]cGMP.

Quantitative Immunoblot Analysis of $P\gamma$ Concentration in ROS—Samples for $P\gamma$ analysis were added to electrophoresis sample buffer, and then subjected to SDS-polyacrylamide gel electrophoresis. After electrophoretic transfer to a 0.45- μm nitrocellulose membrane, the presence of $P\gamma$ was detected with an affinity-purified rabbit polyclonal antibody (UNH9710-4P; 1:15,000 dilution) specific for amino acid residues 63–87 of bovine rod $P\gamma$. (Frog (*Rana pipiens*) $P\gamma$ has an identical amino acid sequence to bovine $P\gamma$ in this region.²) Binding of the $P\gamma$ antibody was determined using a goat anti-rabbit antibody coupled to horseradish peroxidase (1:4000 dilution), followed by incubation of the membrane with substrate (SuperSignal West Pico Chemiluminescent Substrate, Pierce) and luminescent detection on film (Kodak BioMax Light). The intensity of the $P\gamma$ immunoreactive bands was recorded using a scanner and analyzed using the image analysis program, Quantiscan (Biosoft). The concentration of $P\gamma$ in ROS samples was calculated by comparison to a standard curve generated with known amounts (0.5–15 ng) of recombinant $P\gamma$ on the same blot, as described in detail elsewhere (40).

PDE Activity Assay—The rate of cGMP hydrolysis catalyzed by non-activated and activated forms of PDE was measured by a coupled-enzyme phosphate release assay, as described in detail in Ref. 40. Activity measurements were made in the following buffer: 100 mM Tris, 10 mM MgCl_2 , 0.5 mM EDTA, 2 mM dithiothreitol, 0.5 mg/ml bovine

² W. Baehr, personal communication.

TABLE I

Equilibrium and kinetic parameters for high affinity cGMP binding to frog PDE

Binding of [³H]cGMP to nPDE and taPDE were performed at 4 °C as described under "Experimental Procedures." ROS homogenates were depleted of nucleoside phosphates prior to use. Values represent the mean ± S.E. for the number of determinations shown in parentheses.

	K_D (obs.) ^a	k_{-1} ^b	k_{+1} ^c
	nM	s ⁻¹	M ⁻¹ s ⁻¹
nPDE	8.4 ± 1.8 (5)	3.4 ± 0.2 × 10 ⁻⁴ (7)	7.6 ± 0.8 × 10 ⁴ (6)
taPDE			
Slow	57 ± 9.4 (8)	3.4 ± 1.2 × 10 ⁻⁴ ; 64% (8)	7.8 ± 0.8 × 10 ⁴ (7)
Fast		2.9 ± 0.9 × 10 ⁻³ ; 36% (8)	

^a Equilibrium binding measurements of cGMP to nPDE were performed at 4 °C by mixing PDE (8–11 nM) with 1–400 nM [³H]cGMP and incubating for 30 min. Transducin-activated PDE (8–17 nM) was preincubated with GTPγS (added at a concentration equal to the rhodopsin concentration) for 1 min prior to addition of [³H]cGMP. The B_{\max} obtained from these binding isotherms was 1.73 ± 0.11 and 0.98 ± 0.11 mol of cGMP per mol of PDE for nPDE and taPDE, respectively. A second class of low affinity sites on taPDE was not detected in these experiments (see text).

^b Dissociation rate constants (k_{-1}) were determined as described in Fig. 1. Percentage values represent the proportion of the total binding sites exhibiting rapid or slow cGMP dissociation with taPDE in a two-site fit of the dissociation kinetics.

^c Association rate constants (k_{+1}) were calculated from the k_{obs} values in Fig. 1 using the equation: $k_{+1} = (k_{\text{obs}} - k_{-1})/[cGMP]$, where [cGMP] is the total cGMP concentration and ligand depletion is not significant (63).

serum albumin (pH 7.5). In all cases, rate measurements were obtained from at least three individual time points at saturating cGMP concentrations (10 mM), during which time less than 30% of the substrate was consumed.

Other Methods—SDS-polyacrylamide gel electrophoresis was performed by the method of Laemmli (47) in 15% acrylamide gels. The immunoblotting protocol closely followed standard procedures (48). Fitting of PDE activity data was carried out with nonlinear regression analysis using Sigmaplot. Equilibrium binding data as well as the kinetics of cGMP association and dissociation were analyzed as described in Ref. 40; in all cases, statistical comparisons of one-site versus two-site fits were carried out using KELL (Biosoft) to determine whether PDE exhibited one or two distinct classes of cGMP-binding sites.

RESULTS AND DISCUSSION

Transducin Activation of PDE Converts One Class of Noncatalytic Sites to a Low Affinity, Rapidly Exchanging State—Although it has been reported that transducin activation of photoreceptor PDE leads to changes in cGMP binding to the noncatalytic sites of the enzyme, the regulatory and physiological significance of this process is not well understood. A previous study reported that transducin activation of PDE accelerated cGMP exchange and reduced the binding affinity of cGMP to the noncatalytic sites on the enzyme without a significant reduction in the stoichiometry of binding (44). However, this work was conducted with PDE preparations supplemented with exogenous Pγ subunit that markedly affects the interaction of cGMP with the noncatalytic sites (see below). Therefore, we chose to examine the cGMP-binding properties of nonactivated and transducin-activated PDE in ROS homogenates containing only the endogenous Pγ that is present in rod photoreceptor cells. We carried out equilibrium and kinetic studies at 4 °C to slow the binding reactions for accurate measurements of the rate constants.

Non-activated, nucleotide-depleted PDE (nPDE) in frog ROS homogenates binds cGMP with high affinity and as a single class of noninteracting binding sites at 4 °C ($K_D = 8.4$ nM, $B_{\max} = 1.7$ mol of cGMP per mol of PDE; see Table I). The measured K_D values for cGMP binding to frog nPDE agrees with previous estimates when the temperature dependence of the binding

reaction is taken into account (37). (The B_{\max} of nPDE can be increased to 2.0 by addition of ≤1 Pγ per PDE (see Fig. 2C), suggesting that a small amount of Pγ was lost during preparation of nPDE.) When transducin is activated by addition of GTPγS to illuminated ROS homogenates and then 10–400 nM [³H]cGMP is added, transducin-activated PDE (taPDE) undergoes a 7-fold decrease in binding affinity ($K_D = 57$ nM) and a substantial loss in the number of cGMP-binding sites ($B_{\max} = 1.0$ mol cGMP per mol PDE; Table I). At higher [³H]cGMP concentrations up to 1.3 μM, we detected an additional 0.3 mol of cGMP bound per PDE, but we could not resolve a distinct, second class of binding sites. To improve detection of low affinity cGMP-binding sites, we prepared high specific activity [³²P]cGMP and found that increasing the [³²P]cGMP concentration from 1 to 15 μM results in a progressive ($K_{1/2} \sim 5$ μM) increase in total cGMP binding to taPDE from 1.2 to 1.9 cGMP bound per PDE (data not shown). Low affinity cGMP-binding sites were not detected with nPDE. Thus, activation of PDE by transducin induces heterogeneity in the noncatalytic sites on PDE, with a large decrease in binding affinity at one noncatalytic site and a more modest change at the second site.

Measurements of the rate of cGMP association and dissociation were performed to understand better how transducin activation differentially affects cGMP binding to the two noncatalytic sites of PDE. When PDE is incubated with 1 μM [³H]cGMP, a single class of cGMP-binding sites is resolved (Fig. 1A), and the association rate constant is identical for nPDE and taPDE (Table I). (The low affinity cGMP-binding sites on taPDE (~0.2 cGMP per PDE under these conditions) apparently did not contribute sufficiently to be resolved in Fig. 1A.) Thus, transducin activation does not significantly alter the initial step of cGMP binding to the moderate affinity class of sites on taPDE. The association rate constant for cGMP binding ($k_{+1} = 8 \times 10^4$ M⁻¹ s⁻¹) is approximately 3 orders of magnitude below the diffusion-controlled limit for a simple bimolecular protein-ligand binding reaction (49). Restricted diffusion of cGMP to the binding pocket of the noncatalytic sites may result from binding of Pγ in proximity to the noncatalytic domains on Pαβ (50).

Heterogeneity in the noncatalytic cGMP-binding sites was readily observed (Fig. 1B) when bound [³H]cGMP dissociated from taPDE (but not nPDE), in agreement with previous observations (38, 44, 51). PDE activation accelerates 9-fold the exchange rate of cGMP from approximately 0.4 mol cGMP per mol PDE, probably reflecting the low affinity sites that are not saturated under the conditions of this experiment. The remaining two-thirds of the binding sites (0.8 mol cGMP per mol PDE) dissociate bound [³H]cGMP at the same rate as does nPDE. Thus, a 7-fold change in the K_D of the moderate affinity cGMP-binding sites following transducin activation of PDE fails to significantly affect the dissociation rate constant from these sites. The approximately 1000-fold lowering of cGMP affinity to the second class of sites on taPDE has a relatively modest effect on the dissociation rate constant for this class of noncatalytic sites detected in Fig. 1B.

We conclude that the nonactivated PDE holoenzyme consists of two identical, high affinity cGMP-binding sites. Furthermore, the excellent agreement between the observed K_D and the kinetic K_D value ($k_{-1}/k_{+1} = 4.5$ nM) indicates that the association and dissociation reaction steps measured in Fig. 1 represent the rate-limiting steps for cGMP interaction with the noncatalytic sites on nPDE. Upon transducin activation of PDE, heterogeneity in the noncatalytic sites becomes evident. The moderate affinity noncatalytic site on taPDE ($K_D = 57$ nM) retains the same kinetic rate constants for cGMP association and dissociation as observed for nPDE, indicating that some

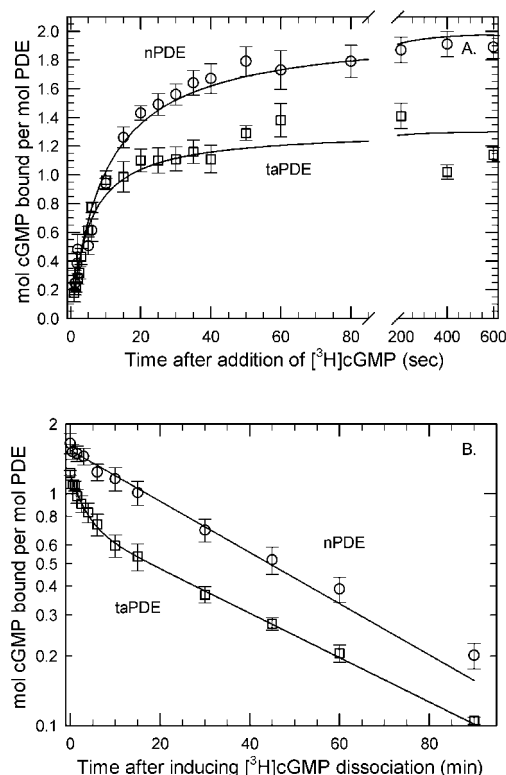


FIG. 1. The kinetics of cGMP exchange at the noncatalytic sites of non-activated and transducin-activated PDE. *A*, for measuring the kinetics of cGMP association to nPDE, 25 nM PDE was mixed with 1 μM [³H]cGMP at 4 °C, and the binding reaction was quenched with ice-cold ammonium sulfate at the indicated times (see “Experimental Procedures”). taPDE was prepared from nPDE by preincubating samples with 1 mM GTP γ S for 1 min prior to cGMP addition. The nPDE data are the mean \pm S.E. for 6 experiments, and the curve is the fit of the data to a pseudo first-order reaction ($k_{\text{obs}} = 7.7 \pm 0.8 \times 10^{-2} \text{ s}^{-1}$; $B_{\text{max}} = 1.83 \pm 0.07$ cGMP bound per PDE). For taPDE, the values are $k_{\text{obs}} = 7.9 \pm 0.8 \times 10^{-2} \text{ s}^{-1}$; $B_{\text{max}} = 1.25 \pm 0.08$ cGMP bound per PDE; $n = 7$. Note that a two-site model was not statistically preferred to the one-site model in all experiments examined. *B*, to measure the kinetics of cGMP dissociation, 60 nM PDE (either non-activated or preincubated for 1 min with GTP γ S as above) was first incubated with 1 μM [³H]cGMP for 30 min at 4 °C to occupy the noncatalytic sites (nPDE, 1.7 cGMP bound per PDE; taPDE, 1.2 cGMP bound per PDE). At time 0, dissociation of [³H]cGMP was initiated by addition of 10 mM unlabeled cGMP, and samples were directly filtered at the indicated times. The data points are the mean \pm S.E. ($n = 6$), and the curves represent the fit of the data to a single exponential for nPDE ($k_{-1} = 3.4 \times 10^{-4} \text{ s}^{-1}$) and a double exponential process for taPDE (36% fast sites, $k_{-1} = 2.9 \times 10^{-3} \text{ s}^{-1}$; 64% slow sites, $k_{-1} = 3.4 \times 10^{-4} \text{ s}^{-1}$).

other rate-limiting process (*e.g.* conformational transition, protein-protein interaction, etc.) must contribute to destabilizing cGMP binding to this class of sites. The low affinity site can only be saturated at high cGMP concentrations (well above micromolar) and represents the small proportion of more rapidly dissociating sites in Fig. 1*B*. The creation of two non-identical cGMP-binding sites upon PDE activation by transducin is likely to result from differences in how α_t -GTP γ S interacts with the α - and β -catalytic subunits.

Exogenous P_{γ} Regulates cGMP Exchange Rates at Both Low and High Affinity Noncatalytic Sites on PDE—To test the role of P_{γ} to regulate cGMP binding to the noncatalytic sites on nPDE and taPDE, we examined whether adding P_{γ} affected cGMP dissociation from nPDE and taPDE. Fig. 2*A* shows that when nPDE is incubated with increasing amounts of P_{γ} and then 1 μM [³H]cGMP is added to occupy the noncatalytic sites, the half-time for [³H]cGMP release is progressively slowed. The ability of P_{γ} to slow cGMP dissociation from nPDE is probably a consequence of reducing (by mass action) the number of PDE

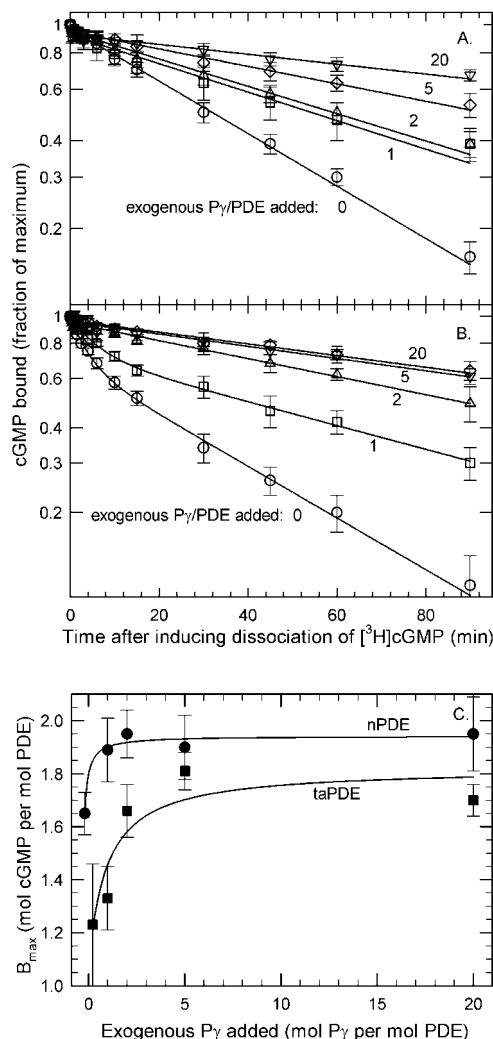


FIG. 2. Effects of exogenous P_{γ} on cGMP dissociation from noncatalytic sites and on the maximum extent of cGMP binding to nPDE and taPDE. ROS homogenates (20 nM PDE, final concentration) were incubated at 4 °C for \sim 4 min with the following concentrations of P_{γ} : 0 (circle), 1.0 (square), 2.0 (triangle), 5.0 (diamond), or 20 (upside-down triangle) mol of P_{γ} per mol of PDE. For transducin-activated PDE (*B*), the ROS were then incubated with 1 mM GTP γ S for 1 min. Following addition of 1 μM [³H]cGMP for 30 min at 4 °C, samples were tested for the maximum extent of cGMP binding (*C*). [³H]cGMP dissociation was initiated upon addition of 10 mM unlabeled cGMP at time 0, and then portions were directly filtered at the indicated times. For nPDE (*A*), the data were best fit to a single exponential decay with the dissociation rates progressively slowing from the control value of $t_{1/2} = 34$ min to a $t_{1/2} = 196$ min for the 20 P_{γ} per PDE condition. For taPDE, a two-site model for the dissociation kinetics was preferred for the 0 and 1 P_{γ} per PDE conditions, with the percentage of the total binding that can be attributed to the “fast” sites diminishing from 35 to $<$ 10% as the amount of added P_{γ} increased from 0 to 2 P_{γ} per PDE. The data are the mean \pm S.E. for three to six determinations of the dissociation rates for each concentration of added P_{γ} .

molecules lacking one or two bound P_{γ} at any moment in time. The sensitivity of cGMP exchange on nPDE to the free P_{γ} concentration suggests a strong allosteric linkage between P_{γ} binding to $P\alpha\beta$ and cGMP occupancy of the noncatalytic sites.

Preincubation of taPDE with increasing amounts of P_{γ} prior to transducin activation has two major effects on the noncatalytic cGMP-binding sites. First, P_{γ} can convert low affinity cGMP-binding sites on taPDE to high affinity sites (Fig. 2*C*). Second, addition of increasing amounts of P_{γ} can reduce (1 P_{γ} added per taPDE) or abolish (\geq 2 P_{γ} added per taPDE) the rapidly dissociating class of noncatalytic sites on taPDE, as well as slowing cGMP dissociation from the other class of sites

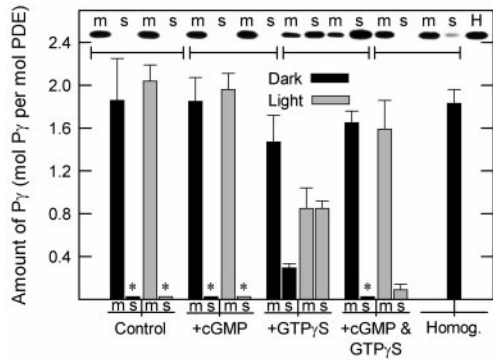


FIG. 3. **P_γ content of membrane and supernatant fractions of frog ROS homogenates.** ROS homogenates (120 nM PDE holoenzyme) in Buffer A were incubated at 4 °C for 30 s with no additions (*Control*), 2.2 mM cGMP (+cGMP), 50 μM GTP_γS (+GTP_γS), or both nucleotides supplemented with 50 μM zaprinast (+cG & GTP_γS). Identical portions were either kept dark-adapted (*black bars*) or exposed to room light (*gray bars*) during the incubation period, and then samples were centrifuged for 1 min at 110,000 × *g* at ambient temperature. Supernatant (*s*) and membrane (*m*) samples were processed on different gels, along with a set of P_γ standards on each gel, to quantitate the P_γ content (see “Experimental Procedures”). Unfractionated, dark-adapted ROS homogenates with no additions (*Homog.*) were also analyzed along with the membrane samples for the sake of comparison. In the representative immunoblot shown in the figure, the supernatant samples were exposed to film for longer times than the membrane samples to permit detection of lower amounts of immunoreactivity. The * indicates that the amount of P_γ was below the level of detection. The data represent the mean ± S.E. for three experiments with different ROS homogenates.

to a similar extent as nPDE (Fig. 2B). It is noteworthy that P_γ exerts these effects on the noncatalytic cGMP-binding sites with greater potency than it can inhibit catalysis at the active site of taPDE (see Fig. 7).

Quantitative Analysis of the P_γ Concentration and Its Subcellular Location in Purified Frog ROS—Because free P_γ greatly affects cGMP binding and exchange kinetics with PDE, we decided to measure the P_γ concentration in intact frog ROS as well as the stoichiometry of P_γ binding to frog Pαβ. By using a quantitative immunoblot procedure, we found that homogenates derived from Percoll-purified frog ROS contained 1.81 ± 0.13 (mean ± S.E.; *n* = 14) mol of P_γ relative to the total concentration of PDE holoenzyme (Fig. 3, *Homog.*). Upon fractionation of these ROS homogenates into membrane and soluble fractions by centrifugation, both dark-adapted and light-exposed ROS retain all P_γ (1.9–2.0 mol P_γ per mol Pαβ) in a membrane-associated state and <0.1 mol P_γ per mol Pαβ in the soluble fractions (Fig. 3, *Control*). The membrane-associated P_γ was bound to PDE, because when frog PDE was released from ROS membranes by hypotonic extraction, a similar stoichiometry of P_γ binding to the released PDE was observed (data not shown).

Addition of cGMP to saturate the noncatalytic sites on PDE did not alter the membrane-associated state or stoichiometry of P_γ binding to dark-adapted or light-exposed PDE (1.9–2.0 mol P_γ per mol Pαβ; Fig. 3, +cGMP). However, if light-exposed ROS homogenates are incubated with GTP_γS to activate transducin, a substantial release of P_γ into the supernatant fraction occurs shortly after nucleotide addition (0.8 ± 0.1 mol P_γ released per mol of Pαβ). This P_γ dissociation into the supernatant can be prevented if millimolar levels of cGMP are included with GTP_γS (0.1 mol P_γ released per mol of Pαβ; Fig. 3). Our quantitative analysis of P_γ agrees with and extends the qualitative observations of Arshavsky *et al.* (39) who first showed that occupancy of the noncatalytic sites by cGMP could prevent P_γ release from ROS membranes following transducin activation.

We conclude that the frog rod PDE holoenzyme consists of a

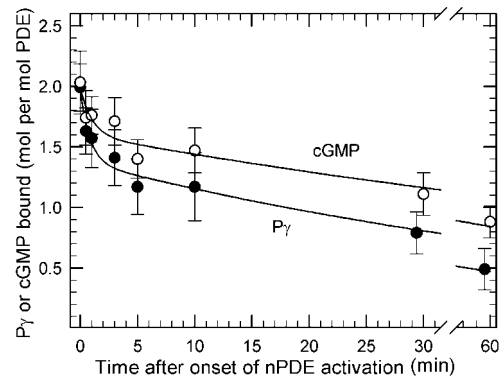


FIG. 4. **P_γ dissociation from transducin-activated PDE correlates with cGMP dissociation from noncatalytic binding sites.** ROS homogenates (30–120 nM PDE) were incubated with 2 μM cGMP or [³H]cGMP and 3 μM E4021 for 10 min at 4 °C. Transducin activation of PDE and dissociation of its bound cGMP was initiated upon addition of 100 μM GTP_γS, 10³ units/liter PDE1, and 8 × 10⁴ units/liter calmodulin (final concentrations). (In control experiments similar to those of Calvert *et al.*, Fig. 5A (51), we determined that PDE1 activities ranging from 500 to 4000 units/liter resulted in identical cGMP dissociation kinetics.) At the indicated times, portions were centrifuged for 1 min at 110,000 × *g* at room temperature. The membrane pellet was then analyzed for either P_γ content (●) or [³H]cGMP binding (○). The data points represent the mean ± S.E. for four experiments where P_γ and [³H]cGMP were both measured on the same preparation. The curves represent the fit of the data to a 2-site binding model as follows: for P_γ release, 30 ± 5% of the P_γ rapidly dissociated (*t*_{1/2} = 0.6 ± 0.2 min) and 70 ± 3% of the P_γ slowly dissociated (*t*_{1/2} = 39 ± 6 min); for cGMP dissociation, 20 ± 7% was rapidly released (*t*_{1/2} = 0.7 ± 0.6 min), whereas 80 ± 5% slowly dissociated (*t*_{1/2} = 65 ± 15 min).

Pαβ catalytic dimer to which 2 P_γ subunits bind, identical to the αβ₂ stoichiometry of membrane-associated bovine rod PDE holoenzyme (52, 53). The absence of P_γ in the ROS cytosol may reflect a tightly regulated, coordinated synthesis of catalytic and inhibitory subunits of PDE (as suggested by P_γ knockout experiments (54)). The fact that approximately 1 mol of P_γ per mol of Pαβ can be released within 1 min of light activation of PDE (Fig. 3, +GTP_γS condition) led us to hypothesize that the state of association of P_γ and cGMP with the PDE holoenzyme may be tightly coupled upon PDE activation by transducin.

cGMP Dissociation from Noncatalytic Sites Correlates with P_γ Release following Transducin Activation of PDE—To test whether cGMP dissociation from noncatalytic sites is directly correlated with P_γ release from taPDE, we examined the time course of cGMP dissociation and of P_γ release following transducin activation of PDE under conditions where the free cGMP concentration was rapidly reduced from its “dark-adapted” concentration (2 μM). To activate PDE and simultaneously lower the free cGMP concentration, we employed a “concentration jump” technique (51) in which GTP_γS was added (to activate frog rod PDE) along with activated PDE1 (to hydrolyze free cGMP rapidly). Release of P_γ and cGMP from PDE were determined by centrifugation of samples through silicone oil and analysis of the pellets for the amount of [³H]cGMP or P_γ bound to the membrane-associated PDE. We found that the time course of cGMP dissociation following transducin activation closely tracked the rate of P_γ release (Fig. 4). Both processes showed biphasic dissociation kinetics, with 20–30% of the reaction occurring rapidly (*t*_{1/2} = 0.6–0.7 min) and the remainder of the dissociation reaction occurring much more slowly (*t*_{1/2} = 40–60 min).

Experimental limitations prevented us from determining the temporal sequence of P_γ and cGMP dissociation from Pαβ. However, it is likely that interaction of α_t-GTP_γS with P_γ bound to the PDE holoenzyme initially displaces P_γ from its

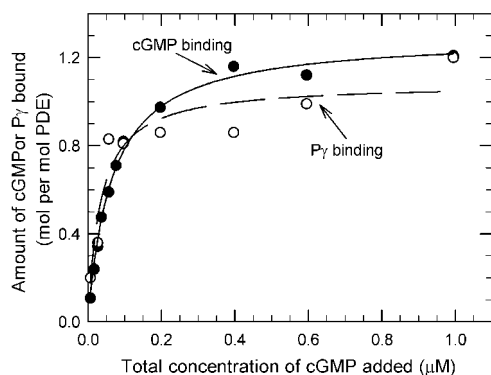


FIG. 5. **Endogenous $P\gamma$ binding to transducin-activated PDE correlates with titration of cGMP binding to the noncatalytic sites.** PDE (15 nM) was transducin-activated by the addition of 10 μ M GTP γ S 1 min prior to the addition of increasing amounts of [3 H]cGMP (with 200 μ M zaprinast). After a 30-min incubation, two portions were quenched into ice-cold buffered ammonium sulfate (see "Experimental Procedures") to determine the [3 H]cGMP content (\bullet). The remaining portion was spun for 1 min at $110,000 \times g$. The supernatants were discarded, and the pellets were washed once and then analyzed for their $P\gamma$ content (\circ). For the cGMP binding data, the curve is a 2-parameter hyperbolic fit with $B_{\max} = 1.3$ cGMP bound per PDE and a $K_D = 65$ nM, whereas the $P\gamma$ binding curve parameters are $B_{\max} = 1.1$ $P\gamma$ per PDE and $K_{1/2} = 34$ nM cGMP. The data shown are representative of 4 individual experiments.

tight association with one catalytic subunit, thereby accelerating cGMP dissociation from the noncatalytic site. Loss of cGMP at this noncatalytic site would further lower the $P\gamma$ binding affinity for $P\alpha\beta$, leading to dissociation of $P\gamma$ - α_t -GTP γ S from $P\alpha\beta$. The observation that cGMP and $P\gamma$ dissociation from the other class of binding sites proceeds as slowly as for nPDE (Fig. 1B) indicates that α_t -GTP γ S is much less effective in binding to the second $P\gamma$ molecule and accelerating cGMP exchange at this noncatalytic site. This might be explained if the remaining $P\gamma$ bound with higher intrinsic affinity to $P\alpha\beta$ than the $P\gamma$ that is rapidly released.

cGMP Occupancy of the Noncatalytic Sites Induces Stoichiometric Binding of $P\gamma$ to taPDE—We next asked whether occupancy of the noncatalytic cGMP-binding sites on taPDE was sufficient to reverse $P\gamma$ dissociation from $P\alpha\beta$. We first prepared taPDE lacking bound cGMP, and we then added increasing concentrations of [3 H]cGMP. After centrifuging the PDE-containing ROS membranes, we simultaneously assayed the extent of [3 H]cGMP binding and the stoichiometry of $P\gamma$ binding to taPDE. Fig. 5 demonstrates a one-to-one correlation between cGMP occupancy of the high affinity noncatalytic sites and $P\gamma$ binding to $P\alpha\beta$. In the absence of cGMP, taPDE bound 0.2 mol of $P\gamma$ per mol of PDE. As increasing concentrations of cGMP were added, taPDE displayed a single class of high affinity cGMP-binding sites ($B_{\max} = 1.3 \pm 0.1$ cGMP bound per PDE; $n = 4$) and a single class of $P\gamma$ -binding sites ($B_{\max} = 1.4 \pm 0.1$ $P\gamma$ bound per PDE; $n = 4$). When incubated with high concentrations of cGMP to occupy both high and low affinity cGMP-binding sites on taPDE, the $P\gamma$ binding stoichiometry approached the same value as for nPDE (Fig. 3, +cGMP & GTP γ S).

We conclude that cGMP occupancy of the noncatalytic sites must induce a conformational change in the $P\alpha\beta$ catalytic dimer that enhances $P\gamma$ binding to $P\alpha\beta$. This allosteric effect of cGMP to enhance $P\gamma$ binding affinity does not act on the C-terminal inhibitory domain of $P\gamma$ (55), because taPDE remains catalytically activated (see below). Rather, a distinct domain on $P\gamma$ (e.g. the central polycationic domain (56)) must be involved in interacting with $P\alpha\beta$ in a cGMP-dependent manner.

Two Distinct Classes of $P\gamma$ -binding Sites on $P\alpha\beta$ Restore

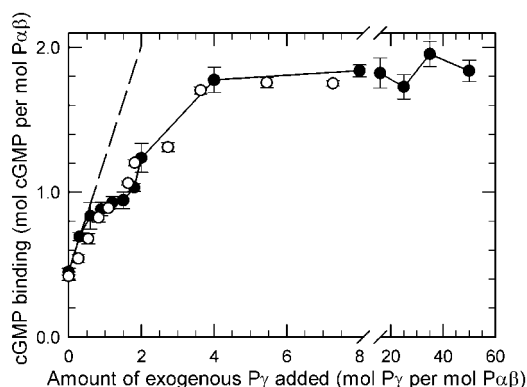


FIG. 6. **The restoration of high affinity cGMP binding to PDE catalytic dimers by $P\gamma$ reveals two classes of binding sites.** Activated PDE was prepared either by extraction of $P\gamma$ from $P\alpha\beta$ by α_t -GTP γ S (\bullet , $n = 5$) or by trypsin proteolysis (2.5 μ g/ml trypsin for 5 min at 4 $^{\circ}$ C) to make tPDE (\circ , $n = 3$), as described under "Experimental Procedures." The residual $P\gamma$ content was $16 \pm 2\%$ for $P\alpha\beta$ and $22 \pm 2\%$ for tPDE. The indicated concentration of $P\gamma$ was incubated with 10 nM $P\alpha\beta$ (\bullet) or 17 nM tPDE (\circ) for 5 min before adding 1 μ M [3 H]cGMP plus 200 μ M zaprinast. The samples were incubated for 30 min at 4 $^{\circ}$ C and then analyzed for the amount of [3 H]cGMP bound to the enzyme. The dashed line represents the results that would have been seen if the restoration of high affinity cGMP binding by $P\gamma$ occurred in a simple one-to-one stoichiometry.

High Affinity cGMP Binding to the Noncatalytic Sites—To understand the basis of the heterogeneity in the noncatalytic sites of taPDE, we needed to study the binding of cGMP and $P\gamma$ to catalytic dimers ($P\alpha\beta$) where $P\gamma$ had been completely removed. Previous work had demonstrated that physical removal of $P\gamma$ from frog rod PDE following transducin activation resulted in a loss of cGMP binding and that addition of $P\gamma$ restored high affinity cGMP binding to noncatalytic sites (36, 44, 57). However, heterogeneity in $P\gamma$ binding to frog $P\alpha\beta$ has been reported in some cases (38, 57) but not in others (36, 44).

Two independent approaches were used to prepare $P\alpha\beta$ catalytic dimers where $P\gamma$ had been removed. The first method is based on the ability of activated transducin to release 50–70% of its $P\gamma$ when the noncatalytic sites are empty (15). (We further optimized the conditions for $P\gamma$ removal from $P\alpha\beta$ to reduce further the amount of $P\gamma$ associated with $P\alpha\beta$ to 10–25% of the original amount (see "Experimental Procedures" and Fig. 4).) The second approach to preparing $P\alpha\beta$ dimers relied on the ability of trypsin proteolysis to degrade $P\gamma$ without adversely affecting the functional properties of $P\alpha\beta$ at its catalytic or noncatalytic sites (43).

Fig. 6 demonstrates that when we prepared $P\alpha\beta$ catalytic dimers by either method, addition of $P\gamma$ to $P\alpha\beta$ in the presence of 1 μ M [3 H]cGMP restores high affinity cGMP binding to the noncatalytic sites in a biphasic manner. Addition of ≤ 1 mol of $P\gamma$ per mol $P\alpha\beta$ results in equimolar cGMP binding to high affinity sites on $P\alpha\beta$. Thereafter, only a slight increase in cGMP binding is observed in the range of 1–2 mol $P\gamma$ added per mol $P\alpha\beta$. It is noteworthy that adding exactly 2 mol of exogenous $P\gamma$ per mol of $P\alpha\beta$ in Fig. 6 leads to the same extent of cGMP binding (1.2 mol cGMP per mol PDE) as is seen for taPDE samples (containing 2 mol of endogenous $P\gamma$ per mol of PDE) under similar conditions (Table I, Fig. 2C, and Fig. 5). Addition of ≥ 4 mol $P\gamma$ per mol $P\alpha\beta$ fully restores cGMP binding to a second class of sites that was unoccupied at lower $P\gamma$ concentrations (consistent with the results in Fig. 2C for taPDE). The results shown in Fig. 6 were also observed when $P\alpha\beta$ was prepared by activating transducin with GTP instead of GTP γ S (data not shown). The data in Fig. 6 are in good agreement with previously published data of Cote *et al.* (44); the more extensive data set and greater precision in determin-

TABLE II
Summary of maximal activities for various preparations of activated frog PDE

PDE preparation ^a	[PDE] ^b	Maximum catalytic activity ^c	<i>n</i>
taPDE	<i>nM</i>	<i>cGMP per s per PDE</i>	
	≥12	4400	Ref. 21
	12–20	4560 ± 140	10
tPDE	0.02	7870 ± 150	Ref. 22
	0.5–3.0	7550 ± 110	23
	15–30	4990 ± 375	5
Pαβ	1–2	7000 ± 180 ^d	8

^a PDE activated by taPDE, trypsin proteolysis (tPDE), or Pγ extraction by α_t-GTPγS (Pαβ) was prepared as described under “Experimental Procedures.”

^b The concentration of PDE used to assay the hydrolytic rate.

^c Determined by measuring catalysis in the presence of saturating levels of cGMP (~100 times the *K_M*). The values are normalized to the concentration of PDE catalytic dimer in each instance.

^d The maximal rate was calculated by correcting the observed rate in each experiment for the residual Pγ (15–25%) remaining bound to Pαβ, assuming a linear dependence of the observed rate with the Pγ content (see Fig. 7).

ing PDE subunit concentrations in Fig. 6 probably account for our ability to resolve the biphasic behavior that was overlooked in the earlier study.

The results in Fig. 6 demonstrate that Pαβ contains two distinct classes of Pγ-binding sites. One class of Pγ-binding sites has very high affinity for Pαβ in the presence of 1 μM cGMP and can bind up to 1 Pγ per Pαβ as a simple titration phenomenon. The noncatalytic cGMP-binding sites that are restored by stoichiometric Pγ addition correspond to the moderate affinity class of sites found in taPDE (Table I and Fig. 5). The second class of Pγ-binding sites on Pαβ is of lower affinity and requires an excess of Pγ (when the cGMP concentration is ≤1 μM) in order to shift the equilibrium to the liganded state. This lower affinity class of Pγ-binding sites is very likely responsible for converting low affinity noncatalytic cGMP-binding sites on taPDE to their high affinity state (Fig. 2C). Although it is probable that the α- and β-catalytic subunits of frog PDE have binding domains for Pγ with intrinsically different binding affinities (as reported for Pγ binding to bovine rod PDE (23)), we cannot rule out allosteric mechanisms that might induce heterogeneity in Pγ binding to Pαβ.

Transducin Activation Fails to Stimulate the Maximum Catalytic Potential of the Pαβ Catalytic Heterodimer—Based on the above results, we hypothesized that heterogeneity in Pγ binding to Pαβ might also result in differences in catalysis at the two active sites on Pαβ. Although most previous work has assumed that each catalytic subunit contributes equally to catalysis upon activation of PDE by transducin, there is wide variation in the reported maximal hydrolytic rates for activated PDE (see Table V in Ref. 2) as well as uncertainty in the stoichiometry and cooperativity of transducin activation of PDE (see Ref. 24 and references therein).

We compared the rates of cGMP hydrolysis for various forms of activated PDE that differed in the method by which the inhibitory constraint of Pγ was relieved. To determine the maximum hydrolytic rate of taPDE, we measured the enzyme activity in light-exposed ROS homogenates following addition of increasing concentrations of GTPγS. Complete activation of PDE by transducin required a concentration of GTPγS sufficient to activate the entire pool of transducin in ROS (data not shown). The *k_{cat}* for taPDE, 4560 ± 140 cGMP/s (Table II) is not significantly different from a previous estimate of 4400 cGMP/s (21).

We used the same frog ROS homogenates to compare directly taPDE with PDE activated by trypsin proteolysis (tPDE). We

found that the *k_{cat}* in the latter case was substantially higher, in contrast to previous comparisons using frog PDE (14, 58). In one set of experiments where we added increasing concentrations of trypsin to 2 nM PDE, we found a maximum catalytic rate of 7640 ± 140 cGMP hydrolyzed per s (*n* = 5; data not shown). In additional experiments where hydrolytic activity measurements were made at relatively low tPDE concentrations (0.5–3 nM PDE), we observed similar high rates (Table II). If hydrolytic activity of tPDE was assayed at substantially higher enzyme concentrations (15–30 nM tPDE), the maximal rate approached the *k_{cat}* for taPDE (Table II). In a separate experiment, progressive dilution of tPDE from 3 to 0.5 nM caused the hydrolytic activity to increase from 6400 to 8100 cGMP/s/PDE; further dilution to 6 pM tPDE had no further effect on the apparent *k_{cat}*. We attribute this phenomenon to the presence of proteolytic fragments of Pγ in our tPDE preparations that retain the ability to bind to and inhibit Pαβ at high, but not low, PDE concentrations. A 4.6-kDa Pγ-immunoreactive band (corresponding to amino acids 46–87 of bovine Pγ (56)) has been detected on immunoblots of tPDE preparations and co-purifies with tPDE following gel filtration chromatography (data not shown).

We have also measured the maximal cGMP hydrolytic rates of Pαβ preparations in which 75–85% of the endogenous Pγ has been extracted by α_t-GTPγS. We find catalytic rates substantially greater (range, 5000–6600 cGMP/s) than the *k_{cat}* for taPDE. When corrected for the residual Pγ content of these Pαβ preparations, the predicted *k_{cat}* of Pαβ dimer devoid of Pγ is 7000 ± 180 cGMP/s (*n* = 8; Table II). Trypsinization of these Pαβ preparations containing residual Pγ can further elevate the hydrolytic rate approximately 25%.

We conclude that the maximum catalytic potential of the Pαβ catalytic dimer approaches 8000 cGMP hydrolyzed per s per Pαβ when all Pγ is released from the enzyme. If we assume each catalytic subunit has the same turnover number (4000 cGMP/s/subunit) and the *K_M* for tPDE is 22 μM (22), the specificity constant *k_{cat}*/*K_M* is calculated to be 1.8 × 10⁸ M⁻¹ s⁻¹. Thus, the catalysis of cGMP into 5'-GMP occurs with extremely high catalytic efficiency and very near the diffusion limit (49). However, PDE never achieves this level of activation *in vivo*, because transducin activation of the enzyme fails to relieve completely Pγ inhibition at both active sites. Rather, α_t-GTPγS acts to relieve completely inhibition at only one of the two active sites on Pαβ, with perhaps a minor (≤10%) effect at the second catalytic site. Activation of PDE catalysis by one, not two, activated transducin molecules in frog ROS homogenates is consistent with the 1:1 stoichiometry of bovine rod PDE activation by transducin in a purified, reconstituted system (24).

Exogenous Pγ Can Stoichiometrically Inhibit Pαβ Catalytic Dimers but Not taPDE—To probe further how transducin binds to and activates the PDE holoenzyme, we examined the ability of exogenous Pγ to inhibit the various forms of activated PDE used in this paper. Previous studies using tPDE or Pαβ preparations offer conflicting views on the ability of Pγ to inhibit activated frog PDE. In some reports, activated PDE can be inhibited by Pγ as a single class of high affinity sites (38, 57), exhibiting the same titration behavior observed with bovine tPDE (e.g. Refs. 11, 43, 59). Other studies with activated frog PDE show evidence for lower affinity Pγ binding and/or complex inhibition of catalysis by added Pγ (14, 15, 36). These differing results may arise from a number of factors, including the concentration of PDE catalytic subunits used, residual Pγ in the activated PDE preparations, and uncertainties in determining the active Pαβ and/or Pγ concentrations.

To resolve these discrepancies, we examined the ability of Pγ

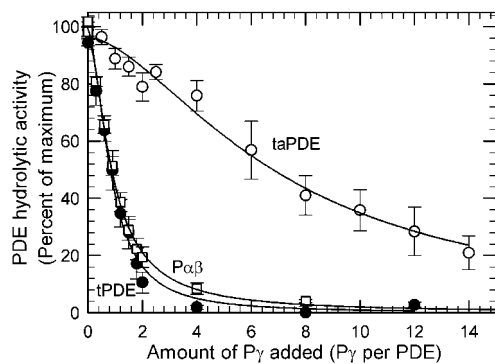


FIG. 7. Stoichiometric $P\gamma$ inhibition of catalysis is observed with tPDE and $P\alpha\beta$ but not with taPDE. tPDE (5 nM) was activated by trypsin treatment (200 $\mu\text{g}/\text{ml}$ trypsin for 10 min at 4 $^{\circ}\text{C}$; see “Experimental Procedures”) and then incubated with the indicated amount of $P\gamma$. taPDE was prepared by first incubating nPDE (30 nM) with the indicated amounts of $P\gamma$ for 2 min prior to addition of 1 mM GTP γ S for 1 min at 22 $^{\circ}\text{C}$. $P\alpha\beta$ dimers depleted of $>70\%$ of its endogenous $P\gamma$ were prepared by two successive extractions of $P\gamma$ with GTP γ S followed by centrifugation (see “Experimental Procedures”). $P\alpha\beta$ (1 nM) was then incubated with the indicated concentrations of exogenous $P\gamma$. PDE catalytic activity was measured with 10 mM cGMP as substrate, and the rates were normalized to the maximum value obtained in the absence of added $P\gamma$. The curves represent a 3-parameter logistic curve fit to the data with IC_{50} values of 0.9, 0.9, and 7.1 $P\gamma$ per PDE for tPDE, $P\alpha\beta$, and taPDE, respectively.

to inhibit activated PDE under conditions where the catalytic and inhibitory subunit concentrations were precisely determined. Fig. 7 shows that PDE activated by transducin responds quite differently to the addition of $P\gamma$ than do tPDE or $P\alpha\beta$ preparations. Both tPDE and $P\alpha\beta$ are stoichiometrically inhibited by 2 mol of $P\gamma$ per mol of $P\alpha\beta$. The steep linear dependence of tPDE and $P\alpha\beta$ activity on the $P\gamma$ concentration reflects a titration phenomenon consistent with the sub-nanomolar binding affinity of $P\gamma$ for frog PDE reported previously (22). The similar behavior for tPDE and $P\alpha\beta$ in Fig. 7 shows that trypsinization of PDE acts primarily on $P\gamma$ and has no noticeable effect on the ability of $P\alpha\beta$ subunits to be inhibited by added $P\gamma$. Although α_t -GTP γ S is present in our $P\alpha\beta$ preparations (see “Experimental Procedures”) and is capable of binding free $P\gamma$ (15), the stoichiometric inhibition of $P\alpha\beta$ by $P\gamma$ demonstrates that α_t -GTP γ S cannot compete effectively with $P\alpha\beta$ for binding to $P\gamma$ under these conditions. Thus, in both instances where activated PDE has had its $P\gamma$ physically removed from the catalytic dimer, exogenous $P\gamma$ has free access to and high affinity for the catalytic sites and can stoichiometrically inhibit catalysis.

In contrast, the inhibition of taPDE by addition of $P\gamma$ requires a greater than 15-fold molar excess of $P\gamma$ to inhibit completely catalytic activity (Fig. 7). The potency of $P\gamma$ inhibition at the active site is severalfold weaker than its ability to convert low affinity noncatalytic binding sites on taPDE to higher affinity sites (Fig. 2C). Note that in the presence of millimolar levels of cGMP in Fig. 7, taPDE binds 2 mol of endogenous $P\gamma$ per mol of PDE (Fig. 3) and has a catalytic activity about one-half of the maximal rate of $P\alpha\beta$ (Table II). It is likely, therefore, that taPDE exists as a complex of α_t -GTP γ S with the PDE holoenzyme. We speculate that a molecule of α_t -GTP γ S, in a complex with $P\gamma$ and a catalytic subunit, hinders the free diffusion of exogenous $P\gamma$ to its inhibitory binding site, thereby reducing the effectiveness of free $P\gamma$ to inhibit cGMP hydrolysis compared with tPDE or $P\alpha\beta$ preparations.

Role of the Noncatalytic cGMP-binding Sites during Transducin Activation of PDE—Our results suggest that the noncatalytic sites on photoreceptor PDE detect changes in cytoplasmic cGMP concentration during phototransduction and

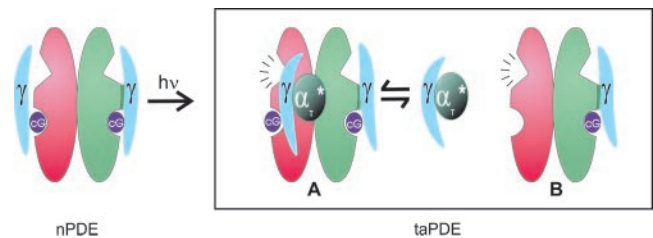


FIG. 8. Model for activation of rod photoreceptor PDE holoenzyme by transducin. The nonactivated form of the PDE holoenzyme (nPDE) is depicted with the right-hand catalytic subunit having a higher affinity for $P\gamma$. Following binding of activated transducin (α_t) to the PDE holoenzyme, the inhibitory constraint of $P\gamma$ is released at the active site (notch) on the left-hand catalytic subunit (lower $P\gamma$ binding affinity). In the presence of high cGMP concentrations, noncatalytic sites (*semi-circles*) remain occupied, and $P\gamma$ remains bound to both subunits (taPDE-A). Lowering the cGMP concentrations causes a transition to taPDE-B in which cGMP dissociates from its low affinity noncatalytic site (*left side*), and $P\gamma$ dissociation accompanies cGMP release. The right-hand subunit of taPDE-B retains bound cGMP and $P\gamma$ because of its intrinsically higher binding affinity for both molecules, and little relief of inhibition occurs at this active site. See text for details.

allosterically regulate the state of association of $P\gamma$ with PDE and with activated transducin. In the dark-adapted state, cGMP levels in rod photoreceptors are much higher ($>1 \mu\text{M}$) than the K_D for cGMP binding to the noncatalytic sites of nPDE. Consequently, $P\gamma$ remains bound to both catalytic subunits in its inhibitory conformation, and cGMP and $P\gamma$ exchange between the bound and free states is expected to be very slow (Fig. 8, nPDE).

Transient light activation of the visual excitation pathway causes activated α_t to displace $P\gamma$ from its inhibitory conformation, and cGMP rapidly drops below micromolar levels. However, the recovery of the dark-adapted state in response to dim flashes (occurring on a time scale of seconds) probably restores cGMP levels (via guanylate cyclase activation) more rapidly than cGMP can dissociate from noncatalytic sites. Under these conditions, activated PDE would consist of a complex of PDE holoenzyme (both noncatalytic sites occupied, both $P\gamma$ bound to $P\alpha\beta$, and one catalytic site fully active; Fig. 8, taPDE-A) and activated α_t . PDE inactivation would depend upon the intrinsic GTPase rate of transducin converting activated α_t -GTP to inactive α_t -GDP.

Persistent activation of the phototransduction cascade by continuous illumination or bright flashes of light causes cytoplasmic cGMP levels to remain below the K_D for the low affinity sites on taPDE long enough for cGMP to dissociate from the low affinity noncatalytic sites. $P\gamma$ dissociation will occur at the same rate because of the highly cooperative nature of $P\gamma$ and cGMP binding to PDE (Fig. 8, taPDE-B). The $P\gamma$ that is released is known to serve as a GTPase-accelerating factor for α_t -GTP, in combination with the Regulator of G-protein Signaling-9 (RGS-9) and the G-protein β_{5L} subunit (60–62). This would speed up transducin inactivation, diminish the amplitude of the light response, and act as a feedback regulator for light adaptation.

Our model predicts that the second catalytic subunit of the PDE holoenzyme remains relatively unaffected by activation of the rod phototransduction cascade, in terms of catalytic activation, $P\gamma$ release, or cGMP dissociation (Fig. 8, right-hand subunit). Only under certain *in vitro* conditions does this subunit undergo changes in ligand binding or catalytic activity. A higher intrinsic affinity of this catalytic subunit for $P\gamma$ may account for this phenomenon.

Additional experiments are needed to test the hypothesis that the noncatalytic sites on PDE serve as a detector of the cGMP concentration in rod photoreceptors during light adaptation. Fu-

ture work will focus on better understanding the properties of the low affinity noncatalytic sites on activated PDE, identifying the structural basis for catalytic subunit heterogeneity, and examining whether the homodimeric cone PDE employs similar regulatory mechanisms in cone photoreceptors.

REFERENCES

- Stryer, L. (1991) *J. Biol. Chem.* **266**, 10711–10714
- Pugh, E. N., Jr., and Lamb, T. D. (1993) *Biochim. Biophys. Acta* **1141**, 111–149
- Helmreich, E. J. M., and Hofmann, K. P. (1996) *Biochim. Biophys. Acta* **1286**, 285–322
- Arshavsky, V. Y., and Pugh, E. N., Jr. (1998) *Neuron* **20**, 11–14
- Loughney, K., Martins, T. J., Harris, E. A. S., Sadhu, K., Hicks, J. B., Sonnenburg, W. K., Beavo, J. A., and Ferguson, K. (1996) *J. Biol. Chem.* **271**, 796–806
- Manganiello, V. C., and Degerman, E. (1999) *Thromb. Haemostasis* **82**, 407–411
- Soderling, S. H., and Beavo, J. A. (2000) *Curr. Opin. Cell Biol.* **12**, 174–179
- Takemoto, D. J., Gonzalez, K., Udovichenko, I., and Cunnick, J. (1993) *Cell. Signal.* **5**, 549–553
- Artemyev, N. O., Arshavsky, V. Y., and Cote, R. H. (1998) *Methods* **14**, 93–104
- Yamazaki, A., Stein, P. J., Chernoff, N., and Bitensky, M. W. (1983) *J. Biol. Chem.* **258**, 8188–8194
- Wensel, T. G., and Stryer, L. (1986) *Proteins Struct. Funct. Genet.* **1**, 90–99
- Bennett, N., and Clerc, A. (1989) *Biochemistry* **28**, 7418–7424
- Bennett, N., Ildefonse, M., Crouzy, S., Chapron, Y., and Clerc, A. (1989) *Proc. Natl. Acad. Sci. U. S. A.* **86**, 3634–3638
- Whalen, M. M., and Bitensky, M. W. (1989) *Biochem. J.* **259**, 13–19
- Yamazaki, A., Hayashi, F., Tatsumi, M., Bitensky, M. W., and George, J. S. (1990) *J. Biol. Chem.* **265**, 11539–11548
- Wensel, T. G., and Stryer, L. (1990) *Biochemistry* **29**, 2155–2161
- Clerc, A., and Bennett, N. (1992) *J. Biol. Chem.* **267**, 6620–6627
- Clerc, A., Catty, P., and Bennett, N. (1992) *J. Biol. Chem.* **267**, 19948–19953
- Otto-Bruc, A., Antonny, B., Vuong, T. M., Chardin, P., and Chabre, M. (1993) *Biochemistry* **32**, 8636–8645
- Bruckert, F., Catty, P., Deterre, P., and Pfister, C. (1994) *Biochemistry* **33**, 12625–12634
- Dumke, C. L., Arshavsky, V. Y., Calvert, P. D., Bownds, M. D., and Pugh, E. N., Jr. (1994) *J. Gen. Physiol.* **103**, 1071–1098
- D'Amours, M. R., and Cote, R. H. (1999) *Biochem. J.* **340**, 863–869
- Berger, A. L., Cerione, R. A., and Erickson, J. W. (1999) *Biochemistry* **38**, 1293–1299
- Melia, T. J., Malinski, J. A., He, F., and Wensel, T. G. (2000) *J. Biol. Chem.* **275**, 3535–3542
- Aravind, L., and Ponting, C. P. (1997) *Trends Biochem. Sci.* **22**, 458–459
- Charbonneau, H., Prusti, R. K., Letrong, H., Sonnenburg, W. K., Mullaney, P. J., Walsh, K. A., and Beavo, J. A. (1990) *Proc. Natl. Acad. Sci. U. S. A.* **87**, 288–292
- McAllister-Lucas, L., Sonnenburg, W. K., Kadlecak, A., Seger, D., Le Trong, H., Colbran, J. L., Thomas, M. K., Walsh, K. A., Francis, S. H., Corbin, J. D., and Beavo, J. A. (1993) *J. Biol. Chem.* **268**, 22863–22873
- Fawcett, L., Baxendale, R., Stacey, P., McGrouther, C., Harrow, I., Soderling, S., Hetman, J., Beavo, J. A., and Phillips, S. C. (2000) *Proc. Natl. Acad. Sci. U. S. A.* **97**, 3702–3707
- Yuasa, K., Kotera, J., Fujishige, K., Michibata, H., Sasaki, T., and Omori, K. (2000) *J. Biol. Chem.* **275**, 31469–31479
- Martins, T. J., Mumby, M. C., and Beavo, J. A. (1982) *J. Biol. Chem.* **257**, 1973–1979
- Yamamoto, T., Manganiello, V. C., and Vaughan, M. (1983) *J. Biol. Chem.* **258**, 12526–12533
- Burns, F., Rodger, I. W., and Pyne, N. J. (1992) *Biochem. J.* **283**, 487–491
- Turko, I. V., Francis, S. H., and Corbin, J. D. (1998) *Biochem. J.* **329**, 505–510
- Corbin, J. D., Turko, I. V., Beasley, A., and Francis, S. H. (2000) *Eur. J. Biochem.* **267**, 2760–2767
- Yamazaki, A., Sen, I., Bitensky, M. W., Casnellie, J. E., and Greengard, P. (1980) *J. Biol. Chem.* **255**, 11619–11624
- Yamazaki, A., Bartucci, F., Ting, A., and Bitensky, M. W. (1982) *Proc. Natl. Acad. Sci. U. S. A.* **79**, 3702–3706
- Cote, R. H., and Brunnock, M. A. (1993) *J. Biol. Chem.* **268**, 17190–17198
- Yamazaki, A., Bondarenko, V. A., Dua, S., Yamazaki, M., Usukura, J., and Hayashi, F. (1996) *J. Biol. Chem.* **271**, 32495–32498
- Arshavsky, V. Y., Dumke, C. L., and Bownds, M. D. (1992) *J. Biol. Chem.* **267**, 24501–24507
- Cote, R. H. (2000) *Methods Enzymol.* **315**, 646–672
- Bownds, M. D., Gordon-Walker, A., Gaido Huguenin, A. C., and Robinson, W. (1971) *J. Gen. Physiol.* **58**, 225–237
- Granovsky, A. E., Muradov, K. G., and Artemyev, N. O. (2000) *Methods Enzymol.* **315**, 635–646
- Mou, H., Grazio, H. J., Cook, T. A., Beavo, J. A., and Cote, R. H. (1999) *J. Biol. Chem.* **274**, 18813–18820
- Cote, R. H., Bownds, M. D., and Arshavsky, V. Y. (1994) *Proc. Natl. Acad. Sci. U. S. A.* **91**, 4845–4849
- D'Amours, M. R., Granovsky, A. E., Artemyev, N. O., and Cote, R. H. (1999) *Mol. Pharmacol.* **55**, 508–514
- Forget, R. S., Martin, J. E., and Cote, R. H. (1993) *Anal. Biochem.* **215**, 159–161
- Laemmli, U. K. (1970) *Nature* **227**, 680–685
- Gallagher, S. (1998) in *Current Protocols in Protein Science* (Coligan, J. E., Dunn, B. M., Ploegh, H. L., Speicher, D. W., and Wingfield, P. T., eds) pp. 10.10.1–10.10.12, John Wiley & Sons, Inc., New York
- Gutfreund, H. (1995) *Kinetics for the Life Sciences: Receptors, Transmitters and Catalysts*, Cambridge University Press, UK
- Natochin, M., and Artemyev, N. O. (1996) *J. Biol. Chem.* **271**, 19964–19969
- Calvert, P. D., Ho, T. W., LeFebvre, Y. M., and Arshavsky, V. Y. (1998) *J. Gen. Physiol.* **111**, 39–51
- Deterre, P., Bigay, J., Forquet, F., Robert, M., and Chabre, M. (1988) *Proc. Natl. Acad. Sci. U. S. A.* **85**, 2424–2428
- Fung, B. K. K., Young, J. H., Yamane, H. K., and Griswold-Prenner, I. (1990) *Biochemistry* **29**, 2657–2664
- Tsang, S. H., Gouras, P., Yamashita, C. K., Kjeldbye, H., Fisher, J., Farber, D. B., and Goff, S. P. (1996) *Science* **272**, 1026–1029
- Granovsky, A. E., Natochin, M., and Artemyev, N. O. (1997) *J. Biol. Chem.* **272**, 11686–11689
- Artemyev, N. O., and Hamm, H. E. (1992) *Biochem. J.* **283**, 273–279
- Yamazaki, A., Yamazaki, M., Bondarenko, V. A., and Matsumoto, H. (1996) *Biochem. Biophys. Res. Commun.* **222**, 488–493
- Whalen, M. M., Bitensky, M. W., and Takemoto, D. J. (1990) *Biochem. J.* **265**, 655–658
- Brown, R. L., and Stryer, L. (1989) *Proc. Natl. Acad. Sci. U. S. A.* **86**, 4922–4926
- Arshavsky, V. Y., and Bownds, M. D. (1992) *Nature* **357**, 416–417
- He, W., Cowan, C. W., and Wensel, T. G. (1998) *Neuron* **20**, 95–102
- Makino, E. R., Handy, J. W., Li, T. S., and Arshavsky, V. Y. (1999) *Proc. Natl. Acad. Sci. U. S. A.* **96**, 1947–1952
- Hulme, E. C., and Birdsall, N. J. M. (1992) in *Receptor-Ligand Interactions: A Practical Approach* (Hulme, E. C., ed) pp. 63–176, Oxford University Press, Oxford
- Hamm, H. E., and Bownds, M. D. (1984) *J. Gen. Physiol.* **84**, 265–280
- Hurley, J. B., and Stryer, L. (1982) *J. Biol. Chem.* **257**, 11094–11099